PROCEEDINGS OF SPIE

SPIEDigitalLibrary.org/conference-proceedings-of-spie

Materials and process development for the fabrication of far ultraviolet device-integrated filters for visible-blind Si sensors

John Hennessy
April D. Jewell
Michael E. Hoenk
David Hitlin
Mickel McClish
Alexander G. Carver
Todd J. Jones
Shouleh Nikzad

SPIE.

Materials and process development for the fabrication of far ultraviolet device-integrated filters for visible-blind Si sensors

John Hennessy[a*], April D. Jewell[a], Michael E. Hoenk[a], David Hitlin[b], Mickel McClish[c], Alexander G. Carver[a], Todd J. Jones[a], Shouleh Nikzad[a]

[a]Jet Propulsion Laboratory, California Insitute of Technology, 4800 Oak Grove Drive, Pasadena, CA, USA 91109; [b]Lauritsen Laboratory, California Institute of Technology, Pasadena, CA, USA 91125; [c]Radiation Monitoring Devices, Inc., 44 Hunt Street, Watertown, MA, USA 02472

ABSTRACT

In this work, we show that the direct integration of ultraviolet metal-dielectric filters with Si sensors can improve throughput over external filter approaches, and yield devices with UV quantum efficiencies greater than 50%, with rejection ratios of visible light greater than 10^3. In order to achieve these efficiencies, two-dimensional doping methods are used to increase the UV sensitivity of back-illuminated Si sensors. Integrated filters are then deposited by a combination of Al evaporation and atomic layer deposition of dielectric spacer layers. At far UV wavelengths these filters require the use of non-absorbing dielectrics, and we have pursued the development of new atomic layer deposition processes for metal fluorides materials of MgF_2, AlF_3 and LiF. The performance of the complete multilayer filters on Si photodiodes and CCD imaging sensors, and the design and fabrication challenges associated with this development are demonstrated. This includes the continued development of deep diffused silicon avalanche photodiodes designed to detect the fast 220 nm emission component of barium fluoride scintillation crystals, while optically rejecting a slower component at 300 nm.

Keywords: ultraviolet, silicon sensor, visible-blind, atomic layer deposition

1. INTRODUCTION

The detection of ultraviolet light often takes in place in the presence of a strong background of visible or solar radiation. For many applications this longer wavelength light is effectively a source of noise, and it is desirable to suppress this signal while maintaining sensitivity in the UV. One approach to accomplish this is through the use of wide-bandgap semiconductor materials in either photoemissive type detectors (*i.e.* photomultiplier tubes or microchannel plates), or in solid-state devices like photodiodes. Photoemissive detectors often possess low quantum efficiencies (< 30%) at UV wavelengths, require high-voltage operation, and are not suitable for use in magnetic fields. Wide-bandgap, visible-blind photodiodes have been demonstrated in materials systems like $Al_{1-x}Ga_xN$ and SiC,[1-3] with demonstrated QE's greater than 50%.[4] However, these devices are often performance-limited by materials quality issues, and are not commonly available in the large arrays needed for high resolution imaging and spectroscopy applications.

Silicon detectors have a more extensive development background drawing on historical advances in the microelectronics industry. A large variety of Si detector devices are commercially available ranging from simple planar photodiodes, avalanche photodiodes (APD), and large-area imaging arrays like CCD or CMOS sensors. These detectors have seen widespread use at visible wavelengths for a large number of consumer, scientific, and industrial applications. Two issues as indicated in Figure 1 have traditionally limited the achievement of high UV sensitivity in Si systems. First, Si possesses a naturally high reflectance at far ultraviolet (FUV, λ=90-200 nm) wavelengths, limiting theoretical QE in this range to 30-40% without the use of anti-reflection coatings. The second issue resulting from the same optical properties, is the shallow absorption depth of FUV photons in Si. When UV photons are absorbed at the surface of Si sensors, the resulting charge carriers can become trapped in surface states that naturally occur at the $Si-SiO_2$ interface, further limiting UV QE.

*john.j.hennessy@jpl.nasa.gov

Image Sensing Technologies: Materials, Devices, Systems, and Applications IV, edited by Nibir K. Dhar, Achyut K. Dutta, Proc. of SPIE Vol. 10209, 102090P

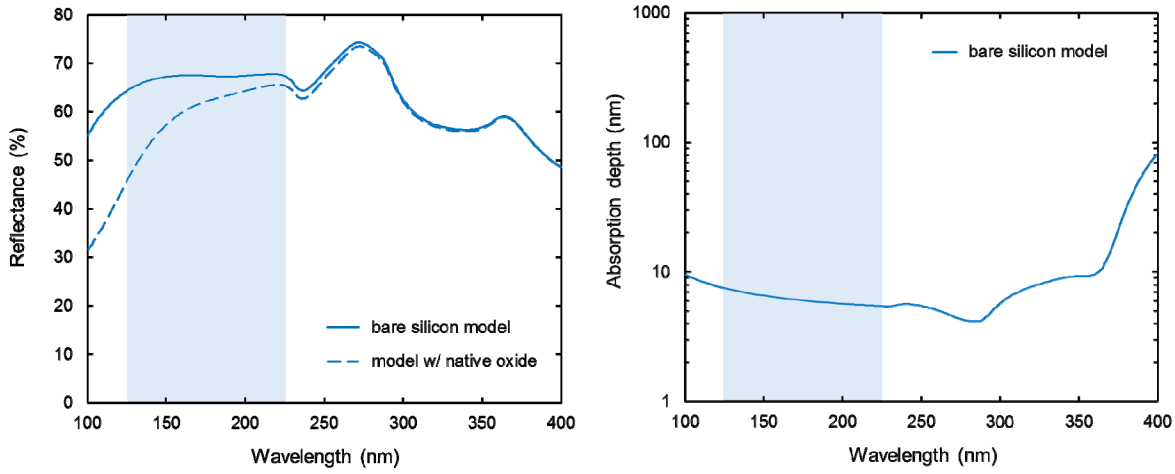

Figure 1. (left) The modeled reflectance of silicon with and without a native oxide layer. (right) The modeled absorption depth of photons in silicon based on the same optical constants. The shaded region highlights wavelengths of interest for this work (~125-225 nm)

The second issue can be addressed through the use of two dimensional (or delta) doping methods developed at JPL. This technique involves the use of molecular beam epitaxy to grow atomically thin, highly doped Si layers on the surface of Si sensors. This modifies the surface electronic band structure to eliminate the trapping effects of surface states. These 2D doping methods have been demonstrated on a variety of Si sensor formats and have been show to achieve 100% internal QE across all UV wavelengths.[5-7] Multiple 2D doped layers (or superlattice structures) can also be employed to provide additional passivation against higher interface state densities.[8]

Additional UV losses from the high reflectance shown in Figure 1 can be recovered in part through the use of anti-reflection coatings.[9] Previous work at JPL has demonstrated CCDs operating at FUV wavelengths with simple single layer AR coatings that can yield QE > 50% across the FUV by combining variable coatings covering 25-50 nm of bandwidth each.[10] Despite the relatively constant reflectance and absorption depth, covering the entire FUV with a single AR coating design is challenging because the refractive index of Si is widely varying in this range. More complex dielectric multilayer structures are typically not available in this range to due to the lack of lossless high-index optical coating materials in the FUV. For example, typical high refractive index optical thin films like HfO_2, TiO_2, and ZnS become strongly absorbing at wavelengths between 250 and 300 nm.

These methods to produce high UV QE in Si sensor platforms also generally maintain high QE throughout the visible portion of the spectrum. In applications where visible or solar blindness is required, selectivity can be obtained via external filtering but the same material challenges become apparent at FUV wavelengths. Complex multilayer dielectric structures are again limited to $\lambda > 250$ nm, and typically lack the bandwidth required to provide blue or UV throughput while simultaneously providing rejection over the entire remaining portion of the Si bandpass. Metal-dielectric filters, or Fabry-Perot filters, operate on a phase-matching interference principle that can provide broad out-of-band rejection. An example of such a filter is illustrated in Figure 2; metallic Al reflector layers are separated by a transparent spacer in order to destructively phase match the reflection and maximize transmission at the design wavelength. When operated at the lowest order (minimum spacer thickness), these filters provide extended out-of-band rejection for wavelengths not subjected to same interference.

Such filters are routinely used in a variety of commercial and space applications where broad long wavelength rejection is required.[11-14] The drawback of such structures is that large rejection ratios require an increasing number of filter cavities, and cumulative losses begin to limit peak UV transmission. For example, commercial bandpass filters can operate with high efficiency (> 60% transmittance) over portions of the near UV (NUV, λ=200-400 nm) spectrum, but generally provide only 10-30% maximum transmittance at FUV wavelengths for out of band rejection ratios greater than 10^3. Even when combined with AR-coated Si sensors, the cumulative system throughput would therefore be limited to approximately 10-20%.

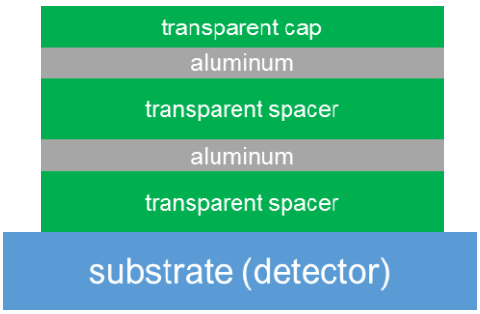

Figure 2. Illustration of a five-layer metal dielectric bandpass filter. For a transparent substrate, this structure forms a single Fabry-Perot cavity. When integrated directly on silicon detector, the reflective substrate now acts as an additional cavity to improve either out-of-band rejection or in-band transmission. In this work aluminum layers form the reflective elements of the traditional Fabry-Perot structure, with deposited transparent dielectric layers as the spacers.

Previous work in our lab has demonstrated that the application of these metal-dielectric filter structures directly onto the Si sensor surface can result in significant performance gains over stand-alone approaches.[15] In this case, the high UV reflectance of Si is beneficial to the performance of the filter structure by acting as an additional partially-matched cavity. Five layer filter structures like the one shown in Figure 2 form an effective double cavity, but without the loss associated with the third reflective layer (now the silicon surface). Initial demonstrations of these filters have been made on 2D-doped Si APDs at a design wavelength near 200 nm utilizing spacer layers of Al_2O_3 deposited by atomic layer deposition (ALD). The subsequent sections of this report describe the development of new ALD processes to extend the performance of these integrated filters to shorter UV wavelengths, the continued optimization and characterization of Al_2O_3-based filters on large area Si APDs for band selective readout devices in a UV scintillation system, and the initial demonstration of AlF_3-based filters on Si CCDs for applications at $\lambda < 200$ nm.

2. ATOMIC LAYER DEPOSITION PROCESS DEVELOPMENT

Our development of metal dielectric device-integrated filters (MDDIF) has relied on the use of ALD to deposit the transparent spacer layers. The use of ALD ensures coating thickness uniformity and repeatability, which is important for the small thicknesses required for UV applications ($\lambda/4 < 50$ nm) and for the coating of large area (> 100 mm diameter) substrates. Previous work at JPL has also demonstrated that ALD is an effective method for preserving the passivating properties of the 2D-doped Si surface. These passivation layers can be damaged by 'energetic' deposition methods like reactive sputtering.[16] ALD processes utilize alternating, self-limiting surface reactions to deposit material one atomic layer at a time. In order to deposit a specific material, the chemistry needed for efficient self-limiting surface reactions must be viable; as opposed to physical vapor deposition methods where the bulk crystal of the desired material can often be used as the source. Many reported ALD dielectric deposition processes are restricted to metal oxide and nitride materials utilizing water vapor as an oxygen source, and ammonia or nitrogen-containing plasmas as a nitrogen source. Aluminum oxide is the most common ALD material and is an appropriate spacer material choice for this MDDIF application at $\lambda > 190$ nm because it is relatively lossless at these wavelengths, and it is index-matched to the oxidation that naturally occurs on the metallic Al layers.

Table 1. Atomic layer deposition processes developed at JPL for ultraviolet fluoride materials utilizing reaction with anhydrous hydrogen fluoride can extend the short wavelength performance of optical thin films deep into the FUV.

HF-BASED METAL FLUORIDE ALD PROCESSES

Material	Co-reactant with Anhydrous HF	$T_{substrate}$ (°C)	~λ Cutoff (nm)
MgF_2	bis(ethylcyclopentadienyl) magnesium	100-250	115-120
AlF_3	trimethylaluminum	100-200	105-110
LiF	lithium bis(trimethylsilyl)amide	100-200	95-100

At shorter wavelengths, lossless dielectric materials are generally limited to metal fluoride thin films, although such materials are less commonly reported by ALD methods. Recent research at JPL has led to the development of several ALD processes for metal fluorides using anhydrous HF as the fluorine-containing precursor.[17,18] The simplicity of this ALD chemistry has enabled the demonstration of the metal fluoride ALD processes indicated in Table 1 at temperature as low as 100 °C, and with reduced impurity concentration and superior UV optical properties. These developments have been employed at JPL in the fabrication of protected aluminum mirrors with coatings of ALD MgF_2, AlF_3, and LiF films.[19-22] This work has a natural extension to Al-based MDDIF structures at FUV wavelengths. Figure 3 shows the measured optical properties of ALD Al_2O_3 compared to ALD AlF_3 highlighting the improvement in the short wavelength cutoff for the fluoride material.

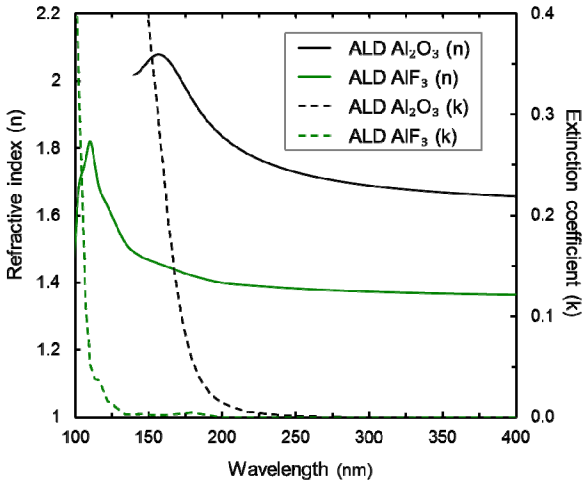

Figure 3. Extracted optical constants for ALD Al_2O_3 and ALD AlF_3. Al_2O_3 was measured by spectroscopic ellipsomtery (SE), AlF_3 was measured by a combination of SE and multi-thickness FUV reflectance measurements at shorter wavelengths. The fluoride material shows a large wavelength reduction in the onset of strong optical absorption.

Another attractive element of the HF-based ALD processing is the possibility to incorporate atomic layer etching (ALE) processes into this MDDIF development to remove the surface oxidation that occurs on the metallic Al layers. The MDDIFs are fabricated with a combination of evaporation for the Al layers and ALD for the dielectric spacers. The intermediate exposure in between each layer allows for some oxidation of the Al layers; this is expected to have little impact at $\lambda > 200$ nm as shown in Figure 3, but becomes increasingly detrimental at FUV wavelengths, especially for multiple cavity filters. Using the same chemistry required for the deposition of ALD AlF_3 can also allow for the ALE of this native Al oxide, and the subsequent capping with AlF_3 within the same vacuum chamber. Protected Al mirrors fabricated with this approach have shown promising results,[23] and we will incorporate this method into our MDDIF development as well.

3. APPLICATION TO SILICON AVALANCHE PHOTODIODES

We have previously reported on the development of Si APDs with MDDIFs for use as a readout device to selectively detect the fast scintillation component of BaF_2 crystals.[8,24,25] This fast scintillation component at 220 nm has potential applications in high rate particle physics calorimetry experiments, but BaF_2 also produces a larger, slower scintillation component at 300 nm. In order to achieve high detection rates, readout devices must therefore suppress this component while maintaining high sensitivity at 220 nm. This objective has been pursued via a collaborative effort between JPL, Caltech, and RMD Inc. Large area (9-14 mm), deep-diffused Si APDs undergo a 2D superlattice doping process at the wafer scale in order to improve UV QE. Following additional processing, a 5 layer MDDIF is also deposited at the wafer scale with a combination of ALD Al_2O_3 and ebeam evaporated Al layers. The blanket MDDIF coating is photolithographically patterned and etched to isolate individual devices. Figure 4 shows a wafer scale image of such devices prior to dicing.

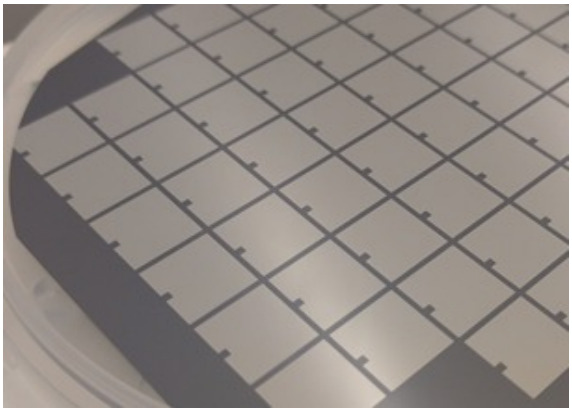

Figure 4. Wafer scale (100 mm) processing of 2D-doped Si APDs with integrated metal dielectric filters. Five layer filter structures composed of Al/Al_2O_3 oxides layers are blanket deposited and post-patterned to isolate individual 9 mm devices.

Performance characterization of MDDIFs is challenging because end-to-end transmission measurements are not possible on non-transmissive detector substrates. Co-deposition on transparent substrates results in a distinctly different interference effect as discussed in previous sections, and therefore still requires correlation with model predictions. At NUV wavelengths we can characterizes the performance of MDDIFs through a combination of spectroscopic ellipsometry (SE) and reflectance measurements. Figure 5 shows an example of a 5 layer (two cavity) MDDIF characterized in this way. Our optical model includes layer thicknesses and refractive index models such as those plotted in Figure 3; this allows for slight variations in effective layer thickness that differ from the target value due to oxidation effects during processing. The model also incorporates secondary effects like Al layer roughness, and interfacial mixing between the metal and dielectric layers. This set of parameters is refined to improve the fit with measured data and refine subsequent MDDIF deposition targets.

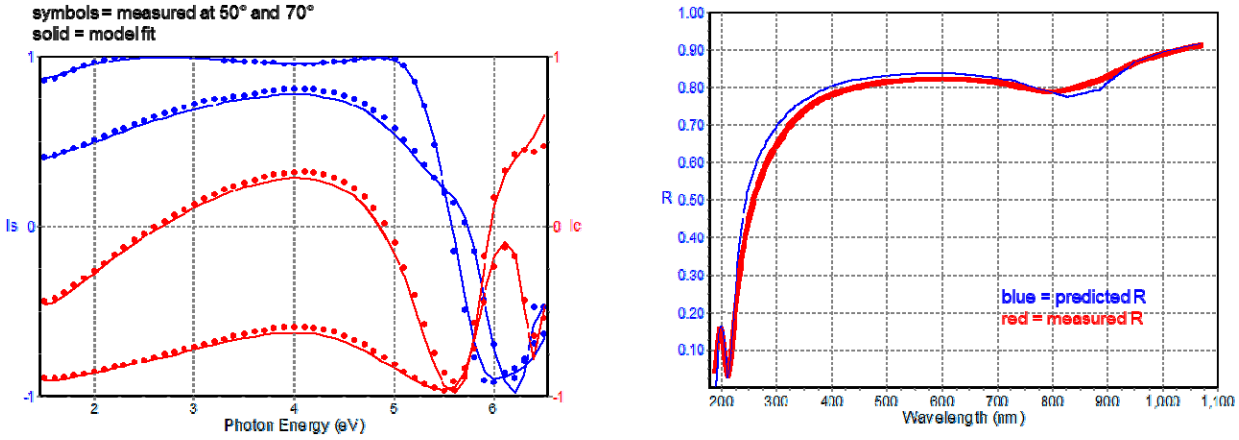

Figure 5. Characterization of five-layer metal dielectric filter deposited directly onto a 2D-doped large-area Si APD. (left) Multi-angle SE measurements show the phase-modulated ellipsometric parameters $I_S = \sin 2\Psi \sin 2\Delta$, and $I_C = \sin 2\Psi \cos 2\Delta$, in comparison to an optical model prediction. (right) The same optical model is simultaneously optimized with measurements of near-normal reflectance to constrain the overall prediction.

This refined model can then be compared directly to spectral measurements of the device QE. Figure 6 shows the measured QE of an APD in comparison the predicted MDDIF transmission target generated from the analysis in Figure 5. For example, this illustrates that the SE and reflectance measurements are able to replicate the slight wavelength shift observed in the completed device response relative to the original performance target. These comparisons are used to adjust layer thickness targets and optical models, and also to evaluate modifications in device process flow to enhance overall transmission. The QE plotted in Figure 6 is scaled relative to the predicted filter transmission by 70%. The QE in these APD devices is measured at unity gain, while the devices are intended to operate at higher biases yielding effective gain factors up to 2000. When operating at high gain the depletion conditions are

distinctly different, and the projected 'effective' QE is higher than that measured at unity gain.[25] In this sense, the 70% scaling factor represents a lower limit to the internal QE of the device and/or the relative transmission of the MDDIF structure. Nevertheless, improvements over previous demonstrations are clear, primarily resulting from reductions in the cumulative thermal budget experienced by the MDDIF structure during processing.

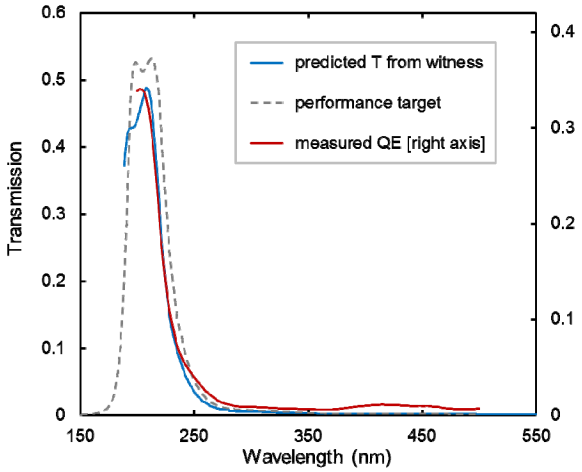

Figure 6. The measured QE (right axis) of 2D superlattice doped Si APDs with 5 layer MDDIFs in comparison the original performance target and the filter transmission predicted from the characterization summarized in Figure 5.

4. APPLICATION TO SILICON IMAGING SENSORS AT FUV WAVELENGTHS

For applications at $\lambda < 190$ nm, alternate spacer materials are required to prevent absorption losses in the MDDIF passband. Preliminary structures base on Al/AlF_3 multilayers have been fabricated on Si CCDs at target wavelengths in the range of 150-175 nm. Figure 7 shows before and after images of a 2D-doped e2V CCD201 device coated with a 5 layer MDDIF. These devices are electron multiplying CCDs with 13 µm pixels in a 1k x 2k format; they are being utilized for variety of FUV imaging and spectroscopy applications at JPL.[26,27] The thinned, back-illuminated devices undergo the 2D-doping process at the wafer scale.[4] Individual devices are isolated following a pad exposure etch process which exposes the wire bond pads from the backside of the wafer prior to dicing. This allows for coating and filter testing at the die level in order to more quickly screen candidate designs. For MDDIF designs it is necessary prevent metal deposition over the bond pads, test devices like the one in Figure 7 are fabricated by physical masking of the Al during evaporation. For future devices where wafer scale processing is possible, the MDDIF can be blanket-deposited and etched back in a manner similar to the APD devices shown in Figure 4.

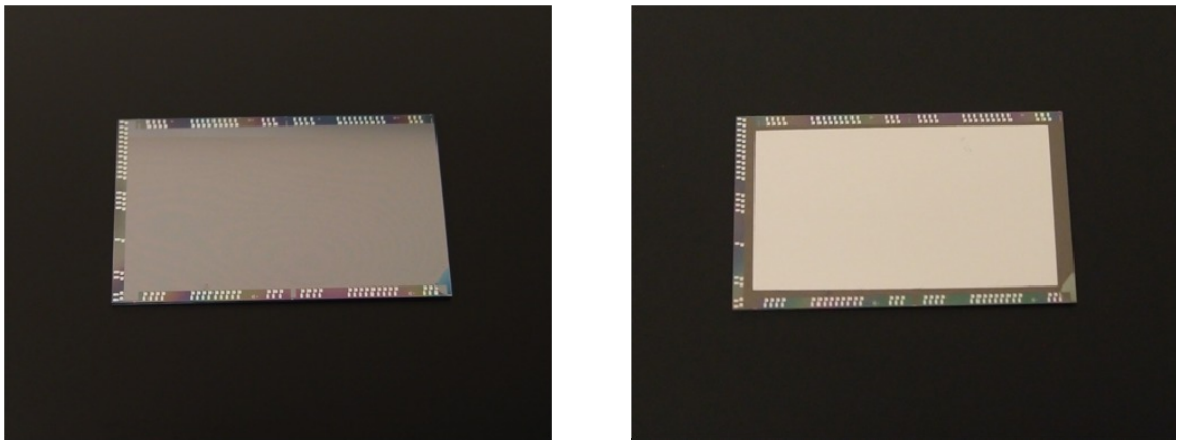

Figure 7. Before and after images of a 2D-doped Si CCD with MDDIF structure of alternating layers of Al and ALD AlF_3.

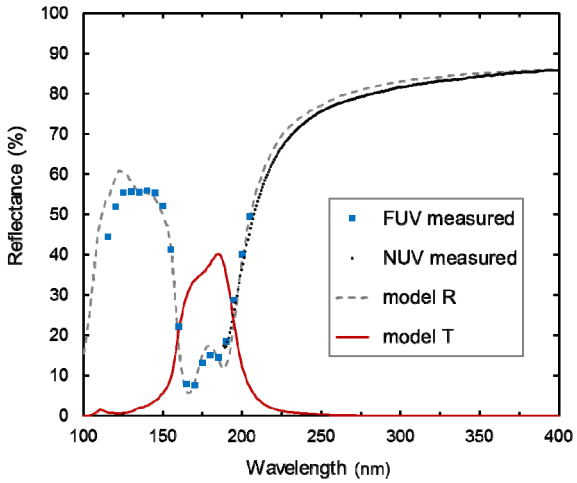

Figure 8. FUV and NUV reflectance characterization of the device pictured in Figure 7 in comparison with a best-fit optical model (dashed line) developed to fit the measured behavior and the corresponding predicted value of transmittance.

Filter characterization becomes more challenging in the FUV due to the lack of in-house SE capabilities below 190 nm, and the additional challenges of precise transmission measurements in this wavelength range. Initial filter performance evaluation has been made with measurements of FUV reflectance as shown in Figure 8. Again, refinement of an optical model is performed to match the measured behavior and predict the filter transmittance. It is noted that the particular device evaluated in Figures 7 and 8 included a thin coating of ALD Al_2O_3 to protect the 2D-doped surface during pad exposure processing. This layer is included in our model in Figure 8 and reduces transmittance by 10-15% at the target bandpass wavelengths. Future devices can be fabricated without this oxide layer or alternatively with an AlF_3 protective layer when processing at the die level. Ongoing work will correlate CCD QE with predicted models in a manner similar to Figure 6, as well as evaluate the impact of MDDIF processing on detector dark current and other device properties.

5. ACKNOWLEDGEMENTS

The research described in this paper was carried out in part at the Jet Propulsion Laboratory, California Institute of Technology, under a contract with the National Aeronautics and Space Administration. APD work was supported by a collaborative effort of Caltech, JPL, and RMD Inc., under SBIR grant DE-SC0011316, and by the Department of Energy. The authors wish to thank K. Balasubramanian at JPL for assistance with the FUV reflectance measurements.

REFERENCES

[1] Suvarna, P., Tungare, M., Leathersich, J.M., Agnihotri, P., Shahedipour-Sandvik, F., Bell, L.D. and Nikzad, S., "Design and growth of visible-blind and solar-blind III-N APDs on sapphire substrates," J. Electron. Mater. 42(5), 854 (2013).

[2] Suvarna, P., Bulmer, J., Leathersich, J.M., Marini, J., Mahaboob, I., Hennessy, J., Bell, L.D., Nikzad, S. and Shahedipour-Sandvik, F., "Ion implantation-based edge termination to improve III-N APD reliability and performance," IEEE Photonics Technol. Lett. 27, 498-501 (2015).

[3] Yan, F., Xin, X., Aslam, S., Zhao, Y., Franz, D., Zhao, J.H. and Weiner, M., "4H-SiC UV photo detectors with large area and very high specific detectivity," IEEE J. Quantum Electron. 40(9), 1315-1320 (2004).

[4] Nikzad, S., Hoenk, M., Jewell, A. D., Hennessy, J., Carver, A. G., Jones, T. J., Goodsall, T. M., Hamden, E. T., Suvarna, P., Bulmer, J., and Shahedipour-Sandvik, F., "Single photon counting UV solar-blind detectors using silicon and III-nitride materials," Sensors 16(6), 927 (2016).

[5] Hoenk, M. E., Grunthaner, P. J., Grunthaner, F. J., Terhune, R. W., Fattahi, M., and Tseng, H.-F., "Growth of a delta-doped silicon layer by molecular beam epitaxy on a charge-coupled device for reflection-limited ultraviolet quantum efficiency," Appl. Phys. Lett. 61, 1084-1086 (1992).

[6] Nikzad, S., Hoenk, M. E., Grunthaner, P. J., Terhune, R. W., Grunthaner, F. J., Winzenread, R., Fattahi, M. M., and Tseng, H.-F., "Delta-doped CCDs for enhanced UV performance," Proc. SPIE 2278, 138-146 (1994).

[7] Nikzad, S., Hoenk, M. E., Grunthaner, P. J., Terhune, R. W., Grunthaner, F. J., Winzenread, R., Fattahi, M. M., Tseng, H.-F., and Lesser, M. P., "Delta-doped CCDs: high QE with long-term stability at UV and visible wavelengths," Proc. SPIE 2198, 907-915 (1994).

[8] Hoenk, M. E., Nikzad, S., Carver, A. G., Jones, T. J., Hennessy, J., Jewell, A. D., Sgro, J., Tsur, S., McClish, M., and Farrell, R., "Superlattice-doped silicon detectors: progress and prospects," Proc. SPIE 9154, 915413 (2014).

[9] Jewell, A. D., Hennessy, J., Hoenk, M. E., and Nikzad, S., "Wide band antireflection coatings deposited by atomic layer deposition," Proc. SPIE 8820, 88200Z (2013).

[10] Nikzad, S., Hoenk, M. E., Greer, F., Jacquot, B., Monacos, S., Jones, T., Blacksberg, J., Hamden, E., Schiminovich, D., Martin, C., and Morrissey, P., "Delta doped electron multiplied CCD with absolute quantum efficiency over 50% in the near to far ultraviolet range for single photon counting applications," Appl. Opt. 51(3), 365-369 (2012).

[11] Trauger, J. T., "Sensors for the Hubble Space Telescope wide field and planetary cameras (1 and 2)," Proc. CCDs in Astronomy 8, 217–230 (1990).

[12] Roming, P. W. A., Kennedy, T. E., Mason, K. O., Nousek, J. A., Ahr, L., Bingham, R. E., Broos, P. S., Carter, M. J., Hancock, B. K., Huckle, H. E., Hunsberger, S. D., Kawakami, H., Killough, R., Koch, T. S., McLelland, M. K., Smith, K., Smith, P. J., Soto, J. C., Boyd, P. T., Breeveld, A. A., Holland, S. T., Ivanushkina, M., Pryzby, M. S., Still, M. D., and Stock, J., "The Swift ultra-violet/optical telescope," Space Sci. Rev. 120, 395–142 (2005).

[13] P. L. Lim, M. Quijada, S. Baggett, J. Biretta, J. MacKenty, R. Boucarut, S. Rice, and J. Del Hoyo, "WFPC2 filters after 16 years on orbit," Bull. Am. Astron. Soc. 43, 254.16 (2011).

[14] Diehl, S., Novotny, R. W., Wohlfahrt, B. and Beck, R., "Readout concepts for the suppression of the slow component of BaF_2 for the upgrade of the TAPS spectrometer at ELSA," J. Phys.: Conf. Ser. 587(1), 012044 (2015).

[15] Hennessy, J., Jewell, A. D., Hoenk, M. E., and Nikzad, S., "Metal–dielectric filters for solar–blind silicon ultraviolet detectors," Appl. Opt. 54, 3507-3512 (2015).

[16] Greer, F., Hamden, E., Jacquot, B. C., Hoenk, M. E., Jones, T. J., Dickie, M. R., Monacos, S. P. and Nikzad, S., "Atomically precise surface engineering of silicon CCDs for enhanced UV quantum efficiency," J. Vac. Sci. Technol. A 31, 01A103 (2013).

[17] Hennessy, J., Jewell, A. D., Greer, F, Lee, M. C., and Nikzad, S., "Atomic layer deposition of magnesium fluoride via bis(ethylcyclopentadienyl)magnesium and anhydrous hydrogen fluoride," J. Vac. Sci. Technol. A 33, 01A125 (2015).

[18] Hennessy, J., Jewell, A. D., Balasubramanian, K., and Nikzad, S., "Ultraviolet optical properties of aluminum fluoride thin films deposited by atomic layer deposition," J. Vac. Sci. Technol. A 34, 01A120 (2016).

[19] Moore, C. S., Hennessy, J., Jewell, A. D., Nikzad, S. and France, K., "Recent developments and results of new ultraviolet reflective mirror coatings," Proc. SPIE 9144, 91444H (2014).

[20] Balasubramanian, K., Hennessy, J., Raouf, N., Nikzad, S., Ayala, M., Shaklan, S., Scowen, P., Del Hoyo, J. and Quijada, M., "Aluminum mirror coatings for UVOIR telescope optics including the far UV," Proc. SPIE 9602, 96020I (2015).

[21] Hennessy, J., Balasubramanian, K., Moore, C. S., Jewell, A. D., Nikzad, S., France, K., and Quijada, M., "Performance and prospects of far ultraviolet aluminum mirrors protected by atomic layer deposition," J. Astron. Telesc. Instrum. Syst. 2(4), 041206 (2016).

[22] Carter, C., Moore, C. S., Hennessy, J., Jewell, A. D., Nikzad, S. and France, K., "Characterizing environmental effects on visible and UV reflectance of ALD-coated optics," Proc. SPIE 9963, 99630V (2016).

[23] Hennessy, J., Moore, C. S., Balasubramanian, K., Jewell, A. D., France, F., and Nikzad, S., "Enhanced atomic layer etching of native aluminum oxide for ultraviolet optical applications," *submitted to J. Vac. Sci. Technol. A*, arXiv:1703.05469 (2017).

[24] Hitlin, D., Kim, J. H., Trevor, J., Hennessy, J., Hoenk, M., Jewell, A., Farrell, R. and McClish, M., "An APD for the detection of the fast scintillation component of BaF_2," IEEE Trans. Nucl. Sci. 63(2), 513-515 (2016).

[25] Nikzad, S., Jewell, A. D., Hoenk, M. E., Jones, T., Hennessy, J., Goodsall, T., Carver, A., Shapiro, C., Cheng, S. R., Hamden, E. and Kyne, G., "High efficiency UV/optical/NIR detectors for large aperture telescopes and UV explorer missions: development of and field observations with delta-doped arrays," *submitted J. Astron. Telesc. Instrum. Syst.*, arXiv:1612.04734 (2016).

[26] Hamden, E. T., Jewell, A. D., Shapiro, C. A., Cheng, S. R., Goodsall, T. M., Hennessy, J., Hoenk, M., Jones, T., Gordon, S., Ong, H. R. and Schiminovich, D., "Charge-coupled devices detectors with high quantum efficiency at UV wavelengths," J. Astron. Telesc. Instrum. Syst. 2(3), 036003 (2016).

[27] Harding, L. K., Demers, R. T., Hoenk, M., Peddada, P., Nemati, B., Cherng, M., Michaels, D., Neat, L. S., Loc, A., Bush, N. and Hall, D., "Technology advancement of the CCD201-20 EMCCD for the WFIRST coronagraph instrument: sensor characterization and radiation damage," J. Astron. Telesc. Instrum. Syst. 2(1), 011007 (2016).